

# Signatures of the Many Supermassive Black Hole Mergers in a Cosmologically Forming Massive Early-Type Galaxy

MATIAS MANNERKOSKI,<sup>1</sup> PETER H. JOHANSSON,<sup>1</sup> ANTTI RANTALA,<sup>2</sup> THORSTEN NAAB,<sup>2</sup> SHIHONG LIAO,<sup>1</sup> AND ALEXANDER RAWLINGS<sup>1</sup>

<sup>1</sup> *Department of Physics, Gustaf Hällströmin katu 2, FI-00014, University of Helsinki, Finland*

<sup>2</sup> *Max-Planck-Institut für Astrophysik, Karl-Schwarzschild-Str 1, D-85748 Garching, Germany*

## ABSTRACT

We model here the merger histories of the supermassive black hole (SMBH) population in the late stages of a cosmological simulation of a  $\sim 2 \times 10^{13} M_{\odot}$  galaxy group. The gravitational dynamics around the several tens of SMBHs ( $M_{\bullet} \gtrsim 7.5 \times 10^7 M_{\odot}$ ) hosted by the galaxies in the group is computed at high accuracy using regularized integration with the KETJU code. The 11 SMBHs which form binaries and hierarchical triplets eventually merge after hardening through dynamical friction, stellar scattering, and gravitational wave (GW) emission. The binaries form at eccentricities of  $e \sim 0.3$ – $0.9$ , with one system evolving to a very high eccentricity of  $e = 0.998$ , and merge on timescales of a few tens to several hundred megayears. During the simulation the merger induced GW recoil kicks eject one SMBH remnant from the central host galaxy. This temporarily drives the galaxy off the  $M_{\bullet}$ – $\sigma_{\star}$  relation, however the galaxy returns to the relation due to subsequent galaxy mergers, which bring in new SMBHs. This showcases a possible mechanism contributing to the observed scatter of the relation. Finally, we show that Pulsar Timing Arrays and LISA would be able to detect parts of the GW signals from the SMBH mergers that occur during the  $\sim 4$  Gyr time span simulated with KETJU.

## 1. INTRODUCTION

The masses of the central supermassive black holes (SMBHs) in massive galaxies are tightly correlated with the structural properties of their host galaxies, which is manifested in the observed  $M_{\bullet}$ – $\sigma_{\star}$  relation (e.g. Kormendy & Ho 2013). During galaxy mergers, SMBHs merge through a three-stage process (Begelman et al. 1980), driven first by dynamical friction until a binary forms, then by three-body scattering between the SMBH binary and individual stars (Hills & Fullerton 1980), and finally at subparsec scales by gravitational wave (GW) emission (Peters 1964).

The GW emission from a binary is in general asymmetric due to the different SMBH masses and spins. This produces a recoil kick, typically giving the merged SMBH a velocity  $\lesssim 500 \text{ km s}^{-1}$ , but reaching  $\sim 4000 \text{ km s}^{-1}$  for suitable spins (e.g. Campanelli et al. 2007). Large kick velocities can significantly displace the merged SMBH or even eject it from the galaxy. This has been suggested to give rise to the observed offset active

galactic nuclei (e.g. Comerford et al. 2015), drive the formation of large galactic cores (Nasim et al. 2021), and contribute to the scatter in the  $M_{\bullet}$ – $\sigma_{\star}$  relation (Blecha et al. 2011).

The GWs emitted during the final phases of an SMBH merger could be detectable by ongoing Pulsar Timing Array (PTA) projects, which primarily target the stochastic superposition of GWs from the expected large number of SMBH binaries (e.g. Arzoumanian et al. 2020) but may also detect individual loud sources. The PTAs are most sensitive to GWs in the nanohertz frequency range and therefore target very massive SMBHs  $M_{\bullet} \gtrsim 10^8 M_{\odot}$  with orbital periods of around a few years (e.g. Kelley et al. 2017). The Laser Interferometer Space Antenna (LISA) (Amaro-Seoane et al. 2017) is a planned space-based detector that will mainly target the GWs emitted during the inspiral and merger of slightly lower mass SMBHs of  $M_{\bullet} \sim 10^6$ – $10^7 M_{\odot}$  up to very high redshifts. However, the final parts of the signals from low-redshift mergers of SMBH binaries with masses around  $M_{\bullet} \sim 10^8 M_{\odot}$  are also expected to be detectable with LISA (Katz & Larson 2019).

In this Letter we study the dynamics of SMBHs and their GW signals in a cosmological zoom-in simulation of a group-sized halo hosting dozens of SMBHs with

Corresponding author: Matias Mannerkoski  
matias.mannerkoski@helsinki.fi

masses  $M_{\bullet} \gtrsim 10^8 M_{\odot}$ . The simulation is run using our updated KETJU code (Rantala et al. 2017, 2018; Mannerkoski et al. 2021), which is able to resolve the dynamics of merging SMBH down to tens of Schwarzschild radii. We now also include a model for GW recoil kicks, which allows us to study the displacement and ejection of SMBHs from their host galaxies.

## 2. NUMERICAL SIMULATIONS

### 2.1. The KETJU Code

The KETJU code extends the widely-used GADGET-3 code (Springel 2005) by replacing the standard leapfrog integration of SMBHs and their surrounding stellar particles with the high-accuracy regularized MSTAR integrator (Rantala et al. 2020) in a small region around each SMBH.

Post-Newtonian (PN) corrections are included in interactions between SMBHs to account for relativistic effects such as GW emission. In addition to binary PN terms, we now also include the leading order 1PN corrections of a general  $N$ -body system, which contain terms involving up to three bodies that may affect the long-term evolution of triplet SMBH systems (Will 2014; Lim & Rodriguez 2020). This is done using the expressions from Thorne & Hartle (1985) for the 1PN and spin terms, whereas higher order corrections valid for BH binary systems up to 3.5PN order are adopted from Eq. (203) of Blanchet (2014).

We now include a model for the mass, spin, and recoil velocity of SMBH merger remnants based on the numerical relativity fitting functions from Zlochower & Lousto (2015). The model uses as inputs the spins and orbital orientation of the BH binary when it is merged at a separation of  $12G(M_1 + M_2)/c^2$ , where  $M_{1,2}$  are the component masses. This gives remnant properties that account for the particular spin directions and orbital orientation of the SMBHs determined by their prior evolution, but which are still only approximate due to the inherent limitations of the fit functions.

We use the same hydrodynamics, star formation, and feedback models as in Mannerkoski et al. (2021), based on the SPHGal smoothed particle hydrodynamics implementation (Hu et al. 2014). Our models include metal-dependent cooling that tracks 11 individual elements, stochastic star formation, feedback from supernovae and massive stars as well as stellar chemical evolution (Scannapieco et al. 2005, 2006; Aumer et al. 2013; Eisenreich et al. 2017). Accretion onto SMBHs is modeled using a simple Bondi–Hoyle–Lyttleton prescription (Johansson et al. 2009b) with thermal feedback on the surrounding gas (Springel et al. 2005). This model successfully produces SMBHs in agreement with the observed scal-

ing relations, but does not correctly model the accretion onto tight binaries or the evolution of SMBH spin. However, these shortcomings are not significant, as the SMBH binaries in this study are mainly found in gas-poor environments and have low accretion rates.

### 2.2. Initial Conditions and Simulations

We run a cosmological zoom-in simulation starting at a redshift  $z = 50$ , targeting a much larger volume than in Mannerkoski et al. (2021). The high-resolution region is centered on a dark matter (DM) halo with a virial mass of  $M_{200} \sim 2.5 \times 10^{13} M_{\odot}$ , covering an initial comoving size of  $(10h^{-1} \text{ Mpc})^3$  and containing  $410^3$  of both gas and DM particles with masses of  $m_{\text{gas}} = 3 \times 10^5 M_{\odot}$  and  $m_{\text{DM}} = 1.6 \times 10^6 M_{\odot}$ . The initial conditions are generated with the MUSIC (Hahn & Abel 2011) software package using the Planck 2018 cosmology (Planck Collaboration et al. 2020) with a Hubble parameter of  $h = 0.674$ .

We first evolve this volume with standard GADGET-3 including SMBH seeding and repositioning until  $z = 0.815$ , at which point the simulation contains tens of galaxies hosting SMBHs with masses  $> 7.5 \times 10^7 M_{\odot}$ . We take this as the lower mass limit of SMBHs to be modeled with KETJU, since a high enough SMBH to stellar particle mass ratio is required to ensure accurate binary dynamics. For this initial run, the gravitational softening lengths were set to  $\epsilon_{\text{bar}} = 40h^{-1} \text{ pc}$  for stars and gas, and  $\epsilon_{\text{DM,high}} = 93h^{-1} \text{ pc}$  for high-resolution dark matter particles.

We continue the run from  $z = 0.815$  with KETJU. For this run, we lower the softening length of the stellar particles to  $\epsilon_{\star} = 20h^{-1} \text{ pc}$  to allow using regularized regions with radii of  $60h^{-1} \text{ pc}$ , resulting in a manageable level of a few thousand stellar particles in each region. At this point we also add spins to the SMBH particles to model their merger recoil kicks. The spin directions are generated from a uniform distribution on the sphere, whereas the spin magnitudes use the distribution from Lousto et al. (2010), resulting in dimensionless spins  $\chi = cJ/GM^2 \sim 0.5\text{--}0.9$ , where  $J$  is the spin angular momentum. Observations constrain the spins of SMBHs with masses above  $10^8 M_{\odot}$  poorly, but are consistent with their spins being in this range (Reynolds 2019). During the simulation, the dimensionless spin may decrease as the gas accretion model does not yet evolve the spin angular momentum.

## 3. RESULTS

### 3.1. Galaxy and SMBH Mergers

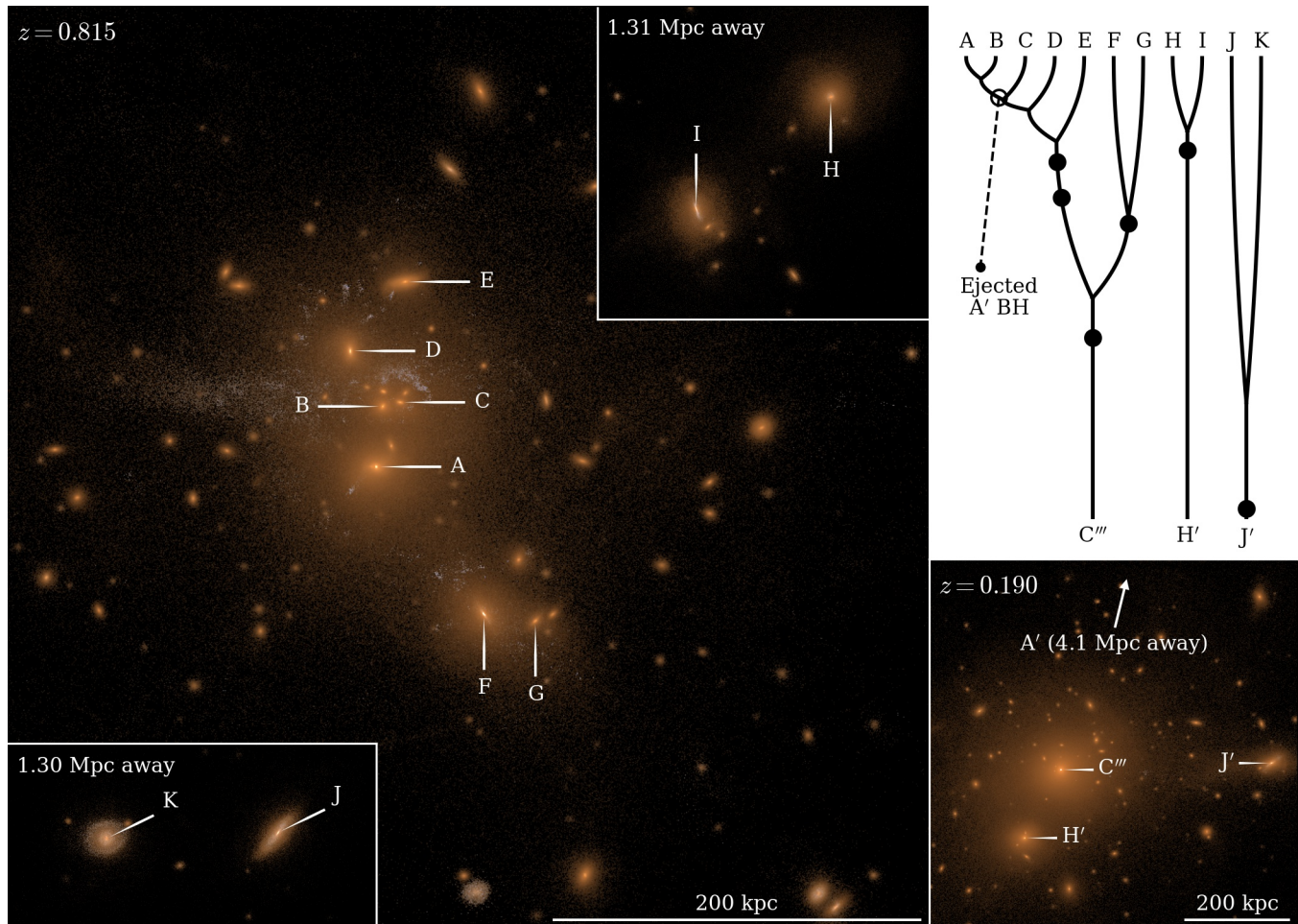


**Figure 1.** Left: The galaxies and SMBHs of interest in the initial state of the KETJU run. The main panel shows the central group of galaxies, with the two more distant pairs of galaxies shown in the corners at the same spatial scale. The images are generated from BVR-luminosities accounting only for stellar emission. Top right: A schematic merger tree of the galaxies and SMBHs with time progressing from top to bottom. The lines follow the galaxy mergers, while the circles indicate SMBH binary mergers. Bottom right: The final state of the simulation with the remaining SMBHs labeled.

At the start of the KETJU simulation there are a total of 11 galaxies hosting massive SMBHs that are involved in mergers over the course of the simulation. These galaxies are shown in the left panel of Figure 1, with the labels marking the locations of the SMBHs (e.g. A), with the host galaxies being referred to as e.g. gA.

Seven of the galaxies (gA–gG) are located in a central group that is collapsing within a halo with a total virial mass of  $M_{200} \approx 2 \times 10^{13} M_{\odot}$  and a virial radius of  $R_{200} \approx 420$  kpc. In addition, there are two pairs of galaxies (gH and gI, gK and gJ) on their initial orbits before merging. They are located within halos of  $M_{200} \approx 2.5 \times 10^{12} M_{\odot}$ ,  $R_{200} \approx 220$  kpc for the gH–gI pair and  $M_{200} \approx 1.3 \times 10^{12} M_{\odot}$ ,  $R_{200} \approx 170$  kpc for the gJ–gK pair. The stellar masses of the galaxies within 30 kpc are  $\sim 5 \times 10^{10} M_{\odot}$ – $3 \times 10^{11} M_{\odot}$  with typical gas fractions of a few percent, except for gG, gJ

and gK which have higher gas fractions of  $\sim 10$ – $25\%$ . Finally, there are another 19 galaxies in the simulation volume, which host SMBHs that are or grow to be massive enough to be modeled with KETJU, as well as a large number of lower mass SMBHs. However, they do not interact with the SMBHs studied here.

As the simulation progresses, the galaxies merge in the order shown in the top right panel of Figure 1. The mergers result in bound SMBH binaries that harden and finally merge due to stellar interactions and GW emission. The evolution of the PN-corrected orbital parameters (Memmesheimer et al. 2004; Mannerkoski et al. 2019) of the binaries is shown in Figure 2, and the properties of the merger remnants are listed in Table 1. The final state of the simulation at  $z = 0.19$  is shown in the lower right panel of Figure 1. The simulation is stopped at this point as there are no more imminent galaxy mergers involving massive SMBHs.



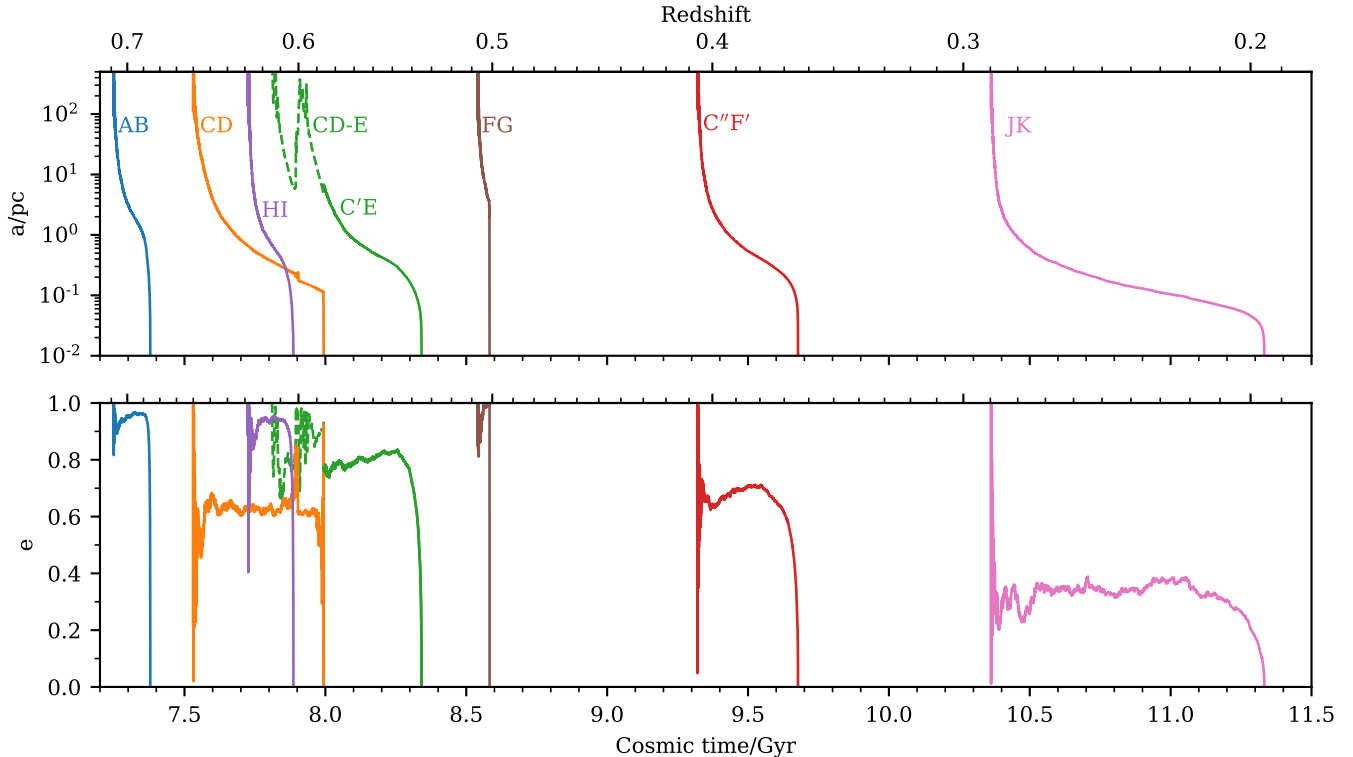


**Figure 2.** Semimajor axis  $a$  (top) and eccentricity  $e$  (bottom) of the SMBH binaries. The dashed line indicates the parameters of the outer orbit in the hierarchical CD-E triplet.

Most of the binaries form at moderately high eccentricities of  $e = 0.6$ – $0.95$ , with little evolution during the hardening process. These high eccentricities result in relatively short binary lifetimes of  $\sim 200$ – $500$  Myr. However, the FG-binary is an exception to this general trend, with a very high peak eccentricity of  $e = 0.998$  resulting in an extremely rapid GW-driven merger in just a few tens of megayears. Another exception is the low-eccentricity ( $e \approx 0.35$ ) JK-binary, which forms after a nearly circular orbit galaxy merger and takes almost a gigayear to merge. The host galaxies gJ and gK are also gas-rich, leading to significant gas accretion onto the SMBHs during the simulation.

Similarly to Mannerkoski et al. (2021), a SMBH triplet also occurs in this simulation (CD-E in Figure 2). However, contrary to our previous study, the outer orbital period is in this case shorter than the relativistic precession period of the inner binary. This results in von Zeipel–Lidov–Kozai type oscillations (Lidov 1962) that eventually excite the CD-binary eccentricity from  $e \approx 0.55$  to a high value of  $e \approx 0.9$ . At the relatively small semimajor axis separation of  $a \approx 0.12$  pc the increased eccentricity is enough to cause a near instant GW driven merger of the CD-binary.

### 3.2. SMBH Ejection and $M_{\bullet}$ – $\sigma_{\star}$ Relation

The SMBH merger remnants mostly experience modest GW recoil kicks of around  $500 \text{ km s}^{-1}$  (Table 1). Such kicks are not strong enough to displace the SMBHs significantly from the centers of their host galaxies, and typically only result in oscillations of  $\sim 200$  pc around the center of the galaxy that are dampened by dynamical friction over a timescale of  $\sim 10$  Myr. The one exception is A', which receives a kick of  $2044 \text{ km s}^{-1}$ . This is above the galactic escape velocity ( $v_{\text{esc}} \sim 1950 \text{ km s}^{-1}$ ) and A' is thus ejected from its host galaxy, receding to a distance of  $4.1 \text{ Mpc}$  by the end of the simulation. While such large kick velocities are in general rare, we find that for this particular SMBH spin configuration, the probability of a kick above  $\gtrsim 2000 \text{ km s}^{-1}$  is about  $\sim 20\%$ .

The ejection of A' leads to an interesting evolution of its host galaxy gA on the  $M_{\bullet}$ – $\sigma_{\star}$  plane, as depicted in Figure 3. This figure also shows the evolution of galaxies gF, gH and gJ which undergo mergers without SMBH ejections. The results from the simulation are compared to the observed relation by Kormendy & Ho (2013),

$$\log\left(\frac{M_{\bullet}}{10^9 M_{\odot}}\right) = -0.51 + 4.38 \log\left(\frac{\sigma_{\star}}{200 \text{ km s}^{-1}}\right), \quad (1)$$

which has an intrinsic scatter of  $\epsilon = 0.29$  in  $\log M_{\bullet}$ .

Initially gA lies within the range expected from the observed relation, but after A' is ejected and C enters

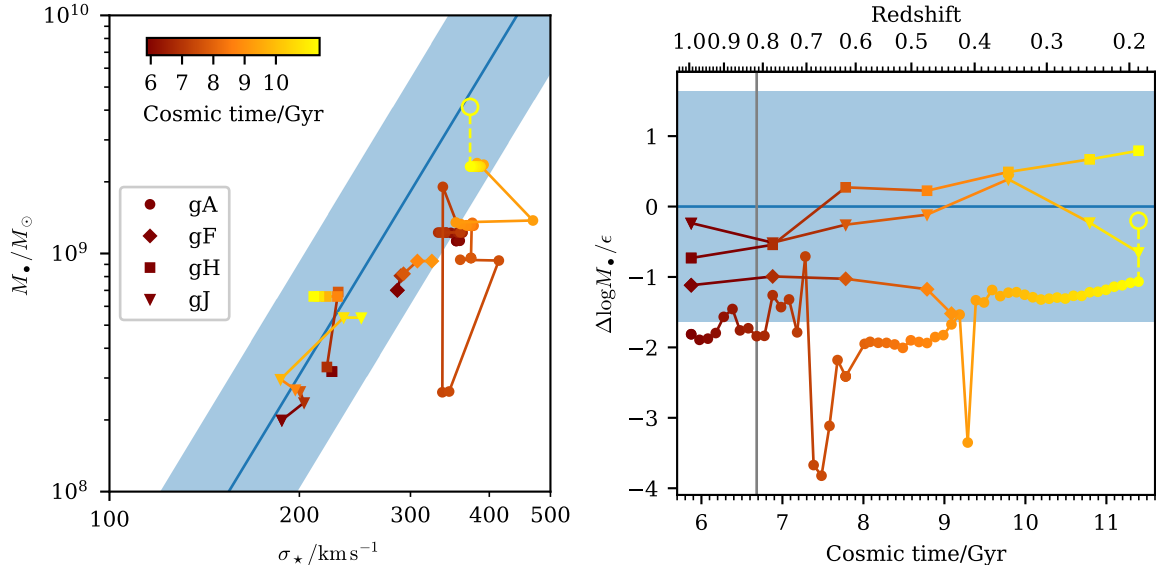


**Figure 3.** Left: The time evolution of galaxies with BH mergers on the  $M_*$ - $\sigma_*$  plane. The line and shaded region show the observed relation (Eq. 1) and the 90% prediction interval corresponding to the intrinsic scatter. The open circle with a dashed line shows where the BH mass would lie without the ejection of A' from the gA-system. In addition to the evolution within the central galaxy gA, the evolution for gF, gH and gJ, which are involved in separate mergers, are shown with a reduced number of data points. Note that gF merges later with gA, thus the data for this system covers a shorter time span. Right: The time evolution of the difference in mass to the relation in units of the intrinsic scatter  $\epsilon$  (see also Johansson et al. 2009a). The vertical line marks the start of the KETJU run.

the galaxy, it becomes significantly offset from the relation at a cosmic time of  $t = 7.5$  Gyr. As galaxies gD and gE merge with gA they bring in their SMBHs, resulting in a partial recovery of the BH mass, with gA moving towards the observed relation. By the end of the simulation the offset falls within the 90% region of the intrinsic scatter of the relation. However, had A' not been ejected, the galaxy and its SMBH would lie even closer to the expected relation as is shown in Figure 3 by the open circle corresponding to a shift by the ejected SMBH mass. In contrast, galaxies gF, gH and gJ evolve following the observed relation after their respective mergers.

### 3.3. Detectability of GW Signals with PTAs

We can estimate whether the GW signal from our simulated SMBH binaries would be individually detectable with PTAs by calculating the signal-to-noise ratio ( $S/N$ ) including the effects of orbital eccentricity using Eq. (65) from Huerta et al. (2015). We use parameter values which resemble values found in currently operating PTAs (e.g. Alam et al. 2021), setting the number of pulsars to  $N_p = 40$ , the observation cadence to  $\Delta t = 0.058$  yr and the timing noise to  $\sigma_{\text{rms}} = 200$  ns. For the duration of observations we choose  $T_{\text{obs}} = 25$  yr, as this increases the detectability of individual systems considerably compared to the current operation time of  $\sim 12$  yr.

The evolution of  $S/N$  values before the mergers of the binaries are shown in the left panel of Figure 4. Following Taylor et al. (2016), binaries with  $S/N$  above  $\sim 5$  might be detectable as resolved sources, meaning that four out of seven SMBH binaries would be detectable starting from  $\sim 10$  Myr before the merger. The other binaries would likely not be individually detectable, but would produce a significant contribution to the GW background.

Unlike circular binaries, which only emit GWs with a frequency  $f = 2f_{\text{orb}}$ , eccentric binaries emit a signal containing all harmonics  $f = nf_{\text{orb}}$  of the orbital frequency. This results in the gradual increase and saw-like oscillation of  $S/N$ , as different harmonics pass through the fairly sharp region of highest sensitivity of the PTA. For the AB and C''F' binaries the signal is detectable already during a period with significant eccentricity, so that  $\sim 1$  Myr prior to the merger the detected GW signal comes from higher harmonics that are not present for a circular binary. In contrast the other binaries only become detectable when the orbits are close to circular and the signal is dominated by the  $n = 2$  harmonic.

### 3.4. Detectability of GW Signals with LISA

The massive SMBH binaries in this study are not prime targets for the planned LISA mission (Amaro-Seoane et al. 2017), as most of their inspiral signal falls below the target frequency sensitivity lower limit

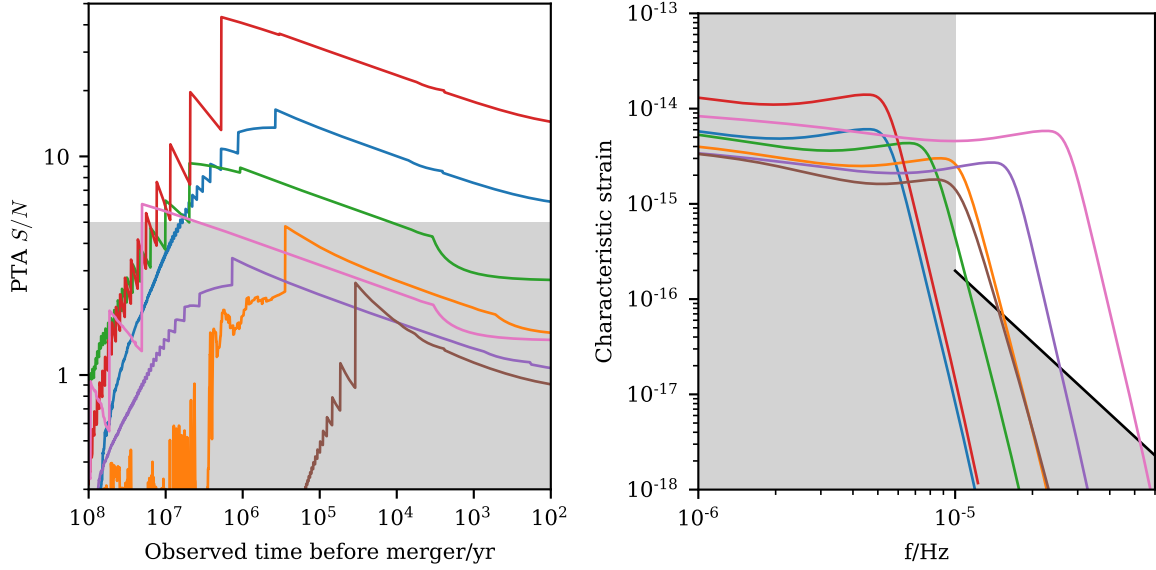


**Figure 4.** Left: The evolution of  $S/N$  observed with PTA as a function of time before the merger. The line colors correspond to different binaries as in Figure 2. The shaded region is likely to be unobservable as resolved targets. Right: The characteristic strain of the binaries during the final stages of their inspiral and merger. The black line shows the planned LISA sensitivity curve. The shaded region is unobservable with the assumed sensitivity.

**Table 1.** Properties of the SMBHs

BH label <sup>a</sup>	$M_{\bullet}/10^8 M_{\odot}$ <sup>b</sup>	$\chi$ <sup>c</sup>	$v_{\text{kick}}/\text{km s}^{-1}$ <sup>d</sup>
A	12.2	0.84	
B	6.7	0.77	
C	2.6	0.63	
D	6.7	0.74	
E	3.3	0.48	
F	7.9	0.79	
G	1.2	0.81	
H	3.3	0.74	
I	3.3	0.58	
J	2.2	0.62	
K	1.1	0.59	
AB $\rightarrow$ A'	18.1	0.67	2044
HI $\rightarrow$ H'	6.6	0.62	171
CD $\rightarrow$ C'	9.6	0.53	474
C'E $\rightarrow$ C''	13.0	0.70	562
FG $\rightarrow$ F'	9.3	0.56	430
C''F' $\rightarrow$ C'''	23.1	0.69	649
JK $\rightarrow$ J'	5.3	0.64	196

<sup>a</sup>Component labels  $\rightarrow$  remnant label for merger remnants.

<sup>b</sup>SMBH mass.

<sup>c</sup>SMBH dimensionless spin parameter.

<sup>d</sup>Merger recoil kick velocity.

of  $f = 2 \times 10^{-5}$  Hz. However, the GW signals from the merger and ringdown phases might still be detectable. In order to test this we calculate the spectra and sky averaged  $S/N$  for our SMBH mergers using the BOWIE code (Katz & Larson 2019) and its implementation of the PhenomD waveform (Husa et al. 2016; Khan et al. 2016).

The right panel of Figure 4 shows the resulting characteristic strain spectra together with the LISA sensitivity curve which is here assumed to extend down to  $f = 10^{-5}$  Hz. The  $S/N$  calculation yields a high value of 410 for the JK-binary merger, which would therefore be easily detectable. The HI merger with  $S/N \sim 55$  would likely also be detectable, while CD and FG mergers with  $S/N \sim 10$  might be detectable if LISA reaches the assumed low frequency sensitivity.

#### 4. CONCLUSIONS

We have demonstrated that the KETJU code can be used to model the small-scale dynamical evolution of dozens of SMBHs in a complex cosmological environment over long periods of time. Seven SMBH binary systems formed during the simulation, and they were all driven to merger by stellar interactions without any signs of stalling (Milosavljević & Merritt 2001). The detailed dynamical evolution of the SMBH binaries naturally depends on how well the central stellar component is resolved. However, it is encouraging that the results obtained here agree well with simulations of similar systems run in isolation at higher spatial resolution (e.g. Rantala et al. 2018; Nasim et al. 2021).

Our simulated SMBH binaries typically formed on quite eccentric orbits, which indicates that circular binary models that have been commonly used in the literature are insufficient for correctly capturing the binary evolution in a majority of the cases. In addition, modeling systems of multiple interacting SMBHs is important for correctly capturing the SMBH merger timescales (e.g. Bonetti et al. 2016), as such situations will naturally occur in a cosmological setting (Mannerkoski et al. 2021). GW recoil kicks of the remnant SMBH will affect its gas accretion history by typically displacing it from the center (Volonteri 2007; Blecha et al. 2011), and in the most extreme case the SMBH can even be completely ejected from its host galaxy. The displacement and ejection of SMBHs will introduce scatter to the observed  $M_{\bullet}-\sigma_{\star}$  relation, but as demonstrated here, it is also possible for a galaxy to recover and evolve back onto the relation under the right circumstances.

Finally, we showed that many of the simulated SMBHs in this study would be potentially detectable with PTAs and LISA, if they had existed in the real Universe at the observed redshifts. In particular PTAs could potentially detect GW signals from the eccentric orbital phase  $\sim 10$  Myr before the merger, whereas LISA would only be able to detect the final stages of the SMBH merg-

ers simulated in this study, given their relatively large masses. Detailed modeling including simultaneously accurate small-scale dynamics and gas physics will be of paramount importance when providing predictions for current and future GW observatories.

M.M., P.H.J., S.L., and A.R. acknowledge the support by the European Research Council via ERC Consolidator Grant KETJU (no. 818930) and the support of the Academy of Finland grant 339127.

T.N. acknowledges support from the Deutsche Forschungsgemeinschaft (DFG, German Research Foundation) under Germany’s Excellence Strategy - EXC-2094 - 390783311 from the DFG Cluster of Excellence “ORIGINS”.

The numerical simulations used computational resources provided by the CSC – IT Center for Science, Finland.

*Software:* KETJU (Rantala et al. 2017, 2020), GADGET-3 (Springel 2005), NumPy (Harris et al. 2020), SciPy (Virtanen et al. 2020), Matplotlib (Hunter 2007), pygad (Röttgers et al. 2020), MUSIC (Hahn & Abel 2011, 2013), BOWIE (Katz & Larson 2019)

## REFERENCES

- Alam, M. F., Arzoumanian, Z., Baker, P. T., et al. 2021, *ApJS*, 252, 5, doi: [10.3847/1538-4365/abc6a1](https://doi.org/10.3847/1538-4365/abc6a1)
- Amaro-Seoane, P., Audley, H., Babak, S., et al. 2017, arXiv e-prints, arXiv:1702.00786. <https://arxiv.org/abs/1702.00786>
- Arzoumanian, Z., Baker, P. T., Blumer, H., et al. 2020, *ApJL*, 905, L34, doi: [10.3847/2041-8213/abd401](https://doi.org/10.3847/2041-8213/abd401)
- Aumer, M., White, S. D. M., Naab, T., & Scannapieco, C. 2013, *MNRAS*, 434, 3142, doi: [10.1093/mnras/stt1230](https://doi.org/10.1093/mnras/stt1230)
- Begelman, M. C., Blandford, R. D., & Rees, M. J. 1980, *Nature*, 287, 307, doi: [10.1038/287307a0](https://doi.org/10.1038/287307a0)
- Blanchet, L. 2014, *Living Reviews in Relativity*, 17, 2, doi: [10.12942/lrr-2014-2](https://doi.org/10.12942/lrr-2014-2)
- Blecha, L., Cox, T. J., Loeb, A., & Hernquist, L. 2011, *MNRAS*, 412, 2154, doi: [10.1111/j.1365-2966.2010.18042.x](https://doi.org/10.1111/j.1365-2966.2010.18042.x)
- Bonetti, M., Haardt, F., Sesana, A., & Barausse, E. 2016, *MNRAS*, 461, 4419, doi: [10.1093/mnras/stw1590](https://doi.org/10.1093/mnras/stw1590)
- Campanelli, M., Lousto, C., Zlochower, Y., & Merritt, D. 2007, *ApJL*, 659, L5, doi: [10.1086/516712](https://doi.org/10.1086/516712)
- Comerford, J. M., Pooley, D., Barrows, R. S., et al. 2015, *ApJ*, 806, 219, doi: [10.1088/0004-637X/806/2/219](https://doi.org/10.1088/0004-637X/806/2/219)
- Eisenreich, M., Naab, T., Choi, E., Ostriker, J. P., & Emsellem, E. 2017, *MNRAS*, 468, 751, doi: [10.1093/mnras/stx473](https://doi.org/10.1093/mnras/stx473)
- Hahn, O., & Abel, T. 2011, *MNRAS*, 415, 2101, doi: [10.1111/j.1365-2966.2011.18820.x](https://doi.org/10.1111/j.1365-2966.2011.18820.x)
- Hahn, O., & Abel, T. 2013, MUSIC: MUlti-Scale Initial Conditions. <http://ascl.net/1311.011>
- Harris, C. R., Millman, K. J., van der Walt, S. J., et al. 2020, *Nature*, 585, 357, doi: [10.1038/s41586-020-2649-2](https://doi.org/10.1038/s41586-020-2649-2)
- Hills, J. G., & Fullerton, L. W. 1980, *AJ*, 85, 1281, doi: [10.1086/112798](https://doi.org/10.1086/112798)
- Hu, C.-Y., Naab, T., Walch, S., Moster, B. P., & Oser, L. 2014, *MNRAS*, 443, 1173, doi: [10.1093/mnras/stu1187](https://doi.org/10.1093/mnras/stu1187)
- Huerta, E. A., McWilliams, S. T., Gair, J. R., & Taylor, S. R. 2015, *PhRvD*, 92, 063010, doi: [10.1103/PhysRevD.92.063010](https://doi.org/10.1103/PhysRevD.92.063010)
- Hunter, J. D. 2007, *Computing in Science and Engineering*, 9, 90, doi: [10.1109/MCSE.2007.55](https://doi.org/10.1109/MCSE.2007.55)
- Husa, S., Khan, S., Hannam, M., et al. 2016, *PhRvD*, 93, 044006, doi: [10.1103/PhysRevD.93.044006](https://doi.org/10.1103/PhysRevD.93.044006)
- Johansson, P. H., Burkert, A., & Naab, T. 2009a, *ApJL*, 707, L184, doi: [10.1088/0004-637X/707/2/L184](https://doi.org/10.1088/0004-637X/707/2/L184)

- Johansson, P. H., Naab, T., & Burkert, A. 2009b, *ApJ*, 690, 802, doi: [10.1088/0004-637X/690/1/802](https://doi.org/10.1088/0004-637X/690/1/802)
- Katz, M. L., & Larson, S. L. 2019, *MNRAS*, 483, 3108, doi: [10.1093/mnras/sty3321](https://doi.org/10.1093/mnras/sty3321)
- Kelley, L. Z., Blecha, L., Hernquist, L., Sesana, A., & Taylor, S. R. 2017, *MNRAS*, 471, 4508, doi: [10.1093/mnras/stx1638](https://doi.org/10.1093/mnras/stx1638)
- Khan, S., Husa, S., Hannam, M., et al. 2016, *PhRvD*, 93, 044007, doi: [10.1103/PhysRevD.93.044007](https://doi.org/10.1103/PhysRevD.93.044007)
- Kormendy, J., & Ho, L. C. 2013, *ARA&A*, 51, 511, doi: [10.1146/annurev-astro-082708-101811](https://doi.org/10.1146/annurev-astro-082708-101811)
- Lidov, M. L. 1962, *Planet. Space Sci.*, 9, 719, doi: [10.1016/0032-0633\(62\)90129-0](https://doi.org/10.1016/0032-0633(62)90129-0)
- Lim, H., & Rodriguez, C. L. 2020, *PhRvD*, 102, 064033, doi: [10.1103/PhysRevD.102.064033](https://doi.org/10.1103/PhysRevD.102.064033)
- Lousto, C. O., Nakano, H., Zlochower, Y., & Campanelli, M. 2010, *PhRvD*, 81, 084023, doi: [10.1103/PhysRevD.81.084023](https://doi.org/10.1103/PhysRevD.81.084023)
- Mannerkoski, M., Johansson, P. H., Pihajoki, P., Rantala, A., & Naab, T. 2019, *ApJ*, 887, 35, doi: [10.3847/1538-4357/ab52f9](https://doi.org/10.3847/1538-4357/ab52f9)
- Mannerkoski, M., Johansson, P. H., Rantala, A., Naab, T., & Liao, S. 2021, *ApJL*, 912, L20, doi: [10.3847/2041-8213/abf9a5](https://doi.org/10.3847/2041-8213/abf9a5)
- Memmesheimer, R.-M., Gopakumar, A., & Schäfer, G. 2004, *PhRvD*, 70, 104011, doi: [10.1103/PhysRevD.70.104011](https://doi.org/10.1103/PhysRevD.70.104011)
- Milosavljević, M., & Merritt, D. 2001, *ApJ*, 563, 34, doi: [10.1086/323830](https://doi.org/10.1086/323830)
- Nasim, I. T., Gualandris, A., Read, J. I., et al. 2021, *MNRAS*, 502, 4794, doi: [10.1093/mnras/stab435](https://doi.org/10.1093/mnras/stab435)
- Peters, P. C. 1964, *Physical Review*, 136, 1224, doi: [10.1103/PhysRev.136.B1224](https://doi.org/10.1103/PhysRev.136.B1224)
- Planck Collaboration, Aghanim, N., Akrami, Y., et al. 2020, *A&A*, 641, A6, doi: [10.1051/0004-6361/201833910](https://doi.org/10.1051/0004-6361/201833910)
- Rantala, A., Johansson, P. H., Naab, T., Thomas, J., & Frigo, M. 2018, *ApJ*, 864, 113, doi: [10.3847/1538-4357/aada47](https://doi.org/10.3847/1538-4357/aada47)
- Rantala, A., Pihajoki, P., Johansson, P. H., et al. 2017, *ApJ*, 840, 53, doi: [10.3847/1538-4357/aa6d65](https://doi.org/10.3847/1538-4357/aa6d65)
- Rantala, A., Pihajoki, P., Mannerkoski, M., Johansson, P. H., & Naab, T. 2020, *MNRAS*, 492, 4131, doi: [10.1093/mnras/staa084](https://doi.org/10.1093/mnras/staa084)
- Reynolds, C. S. 2019, *Nature Astronomy*, 3, 41, doi: [10.1038/s41550-018-0665-z](https://doi.org/10.1038/s41550-018-0665-z)
- Röttgers, B., Naab, T., Cernetic, M., et al. 2020, *MNRAS*, 496, 152, doi: [10.1093/mnras/staa1490](https://doi.org/10.1093/mnras/staa1490)
- Scannapieco, C., Tissera, P. B., White, S. D. M., & Springel, V. 2005, *MNRAS*, 364, 552, doi: [10.1111/j.1365-2966.2005.09574.x](https://doi.org/10.1111/j.1365-2966.2005.09574.x)
- Scannapieco, C., Tissera, P. B., White, S. D. M., & Springel, V. 2006, *MNRAS*, 371, 1125, doi: [10.1111/j.1365-2966.2006.10785.x](https://doi.org/10.1111/j.1365-2966.2006.10785.x)
- Springel, V. 2005, *MNRAS*, 364, 1105, doi: [10.1111/j.1365-2966.2005.09655.x](https://doi.org/10.1111/j.1365-2966.2005.09655.x)
- Springel, V., Di Matteo, T., & Hernquist, L. 2005, *MNRAS*, 361, 776, doi: [10.1111/j.1365-2966.2005.09238.x](https://doi.org/10.1111/j.1365-2966.2005.09238.x)
- Taylor, S. R., Huerta, E. A., Gair, J. R., & McWilliams, S. T. 2016, *ApJ*, 817, 70, doi: [10.3847/0004-637X/817/1/70](https://doi.org/10.3847/0004-637X/817/1/70)
- Thorne, K. S., & Hartle, J. B. 1985, *PhRvD*, 31, 1815, doi: [10.1103/PhysRevD.31.1815](https://doi.org/10.1103/PhysRevD.31.1815)
- Virtanen, P., Gommers, R., Oliphant, T. E., et al. 2020, *Nature Methods*, 17, 261, doi: [10.1038/s41592-019-0686-2](https://doi.org/10.1038/s41592-019-0686-2)
- Volonteri, M. 2007, *ApJL*, 663, L5, doi: [10.1086/519525](https://doi.org/10.1086/519525)
- Will, C. M. 2014, *PhRvD*, 89, 044043, doi: [10.1103/PhysRevD.89.044043](https://doi.org/10.1103/PhysRevD.89.044043)
- Zlochower, Y., & Lousto, C. O. 2015, *PhRvD*, 92, 024022, doi: [10.1103/PhysRevD.92.024022](https://doi.org/10.1103/PhysRevD.92.024022)